Prediction algorithms for real-time respiratory motion monitoring

Florian Aymanns

Group leader: Prof. Dr. Antony John Lomax
Supervisor: Dr. Giovanni Fattori

May 2016

Abstract

In this work the use of polynomial, wavelet based and support vector regression methods were investigated for respiratory signal prediction. Geometrical and temporal accuracy of predicted motion trajectories were evaluated considering root mean square error (RMSE), jitter and phase shift metrics. Second order polynomial prediction outperforms the other algorithms with a maximal RMSE of $\sim 0.09mm$ and ~ 1.1 relative jitter. Polynomial algorithms were further applied for on-line detection of singular points characteristic of motion signals, i.e. full inhale peaks and end exhale plateaux. Finally, polynomial and wavelet approaches were implemented in C to perform accurate code profiling, resulting in respectively $\sim 3\mu s$ and $\sim 8\mu s$ execution time.

Contents

1 Introduction

The precision of proton therapy in thoracic and abdominal treatment sites is limited by respiration induced organ motion. Its accurate monitoring prior and during treatment is a key aspect for the implementation of motion mitigation strategies, either based on beam gating or tumour tracking. For motion monitoring, optical based solutions are often applied in clinical practice, having the advantage of being non-invasive. However, systematic latencies occur from motion observation to motion mitigation with the treatment delivery system. As such, motion prediction algorithms need to be applied to achieve effective real time motion detection.
A simple approach to signal prediction is based on causal filters, whose output depends on present and past samples in agreement with the following definition:

$$y(t+\delta) = f(y(t), y(t-1), y(t-2), ..., y(t-N)) \quad (1)$$

where δ is the prediction horizon and N the signal history considered for the prediction. Based on the input the algorithm is trained independently of the horizon (training step), before the actual prediction is performed (prediction step).

Aim of this project The algorithms' performance was evaluated in terms of geometrical and temporal accuracy of predicted motion trajectories considering root mean square error (RMSE), jitter and phase shift metrics. In addition, polynomial algorithms were applied for on-line detection of singular points characteristic of respiratory motion signals, i.e. full inhale peaks and end exhale plateaux. Finally, in the perspective of including motion prediction in the PSI specific solution for respiratory gating [5], a selected set of algorithms was implemented in C to perform accurate code profiling.

1.1 Polynomial signal prediction

The polynomial prediction is the simplest approach investigated. It basically reduces the training step to polynomial fitting of the signal history. In the consecutive prediction part this polynomial is simply evaluated at arbitrary future time instants ($t_0 + t_{horizon}$). For second order polynomials the prediction step is shown in equation 2, where the coefficients α, β, γ are the best fitting for the system of equations 3 in least-squares sense. This study is limited to first and second degree polynomials, to prevent the overfit of signal noise.

$$y(t_n + t_{horizon}) = \alpha(t_n + t_{horizon})^2 + \beta(t_n + t_{horizon}) + \gamma \tag{2}$$

$$y_i = \alpha t_i^2 + \beta t_i + \gamma, \quad i = n, ..., n - N_{hist} \tag{3}$$

1.2 Wavelet based signal prediction

Just like the polynomial prediction, the **w**avelet based prediction is also based on a **L**east **M**ean **S**quares optimization (wLMS). Only a very brief description of the algorithm is given here. The reader is referred to Ernst et al. 2012 [3] and Renaud et al. 2003 [9] for further details.
The first step for wLMS signal prediction consists of the "à trous" wavelet decomposition of the signal history to compute the wavelet scale parameters ($W_1, ..., W_J$) and the smoothed signal c_J. The decomposition satisfies

N_{hist}	length of the history used to compute the wavelet decomposition $N_{hist} \geq k + M - 1 + max\{\{2^j(a_j \ - 1),\ j = 1, ..., J\} \cup \{2^J(a_{J+1} \ - 1)\}\}$
J	number of scales
M	number of rows in matrix B, with $Bw = (y_n, ..., y_{n-M+1})^T$ can be interpreted as the number of histories used for least-squares optimisation
k	prediction horizon in samples
μ	averaging parameter $w_{m+1} = (1-\mu)w_n + \mu B^+(y_n, ..., y_{n-M+1})^T$

Table 1: Parameters of the wLMS and their description.

equation 4.

$$y_n = W_{1,n} + ... + W_{J,n} + c_{J,n} \tag{4}$$

The final prediction step is given by:

$$y_{n+k} = \sum_{j=1}^{J} w_{n,j}^T \tilde{W}_{n,j} + w_{J+1}^T \tilde{c}, \tag{5}$$

where $\tilde{W}_{n,j}$ and $\tilde{c}_n$ are given by equations 6.

$$\begin{aligned} \tilde{W}_{n,j} &= (W_{j,n-2^j \cdot 0}, W_{j,n-2^j \cdot 1}, ..., W_{j,n-2^j \cdot (a_j - 1)})^T \\ \tilde{c}_n &= (c_{J,n-2^J \cdot 0}, c_{J,n-2^J \cdot 1}, ..., c_{J,n-2^J \cdot (a_J - 1)})^T \end{aligned} \tag{6}$$

a_1 and a_2 parameters defining the regression depths were set to 0 in order to reduce noise on the predicted signal. For the calculation of the wavelet weights $w_{n,j}$ and w_{J+1} a pseudo inverse was used. The list of parameters that have to be set for the wLMS algorithms are shown in Table 1.

1.3 Support vector regression signal prediction

Support **V**ector **R**egression (SVR) is a regression technique derived from the support vector classification methods formulized in machine learning. Its peculiarity consists of considering only the subset of most relevant training data samples to build the regression model thus improving the prediction accuracy. However, the high computational cost of its original formulation limits its adoption in real-time applications. The fastest implementation

ϵ	Distance threshold for penalisation. Data points y_i with $\lvert f(x) - y_i \rvert < \epsilon$ are penalised in the optimisation.
C	Influences the strength of penalisation. Coefficient of so called slack variable in the Lagrangian.
Kernel type	A Kernel function is needed for non-linear regression problems. It maps the input in to a feature space.
Kernel parameter	Parameter that specifies the the shape of the kernel function. Also multiple kernel parameters of none are possible depending on the kernel function used.
N_{hist}	history length
$t_{horizon}$	prediction horizon in msec

Table 2: Parameters of the AOSVR and their description.

available has been detailed by Ma et al. in 2003 [7], namely the accurate on-line support vector regression (AOSVR). The list of most relevant parameters is listed in Table 2. For further information the reader is referred to Ernst et al. 2009 [4], that discuss SVR with specific focus on respiratory motion prediction. Similarly to Ernst and Schweikard's approach [4], in our implementation we have choosen a Gaussian radial basis function as kernel function. Equation 7 shows the Gaussian radial basis function with the kernel parameter σ used in our implementation [8].

$$K(x,y) = e^{\frac{-|x-y|^2}{2\sigma^2}} \tag{7}$$

2 Latency compensation: time prediction of respiratory motion

The evaluation of algorithms' performance is based on the comparison between the output of the prediction model and a reference trajectory obtained by shifting model input by the amount of prediction applied. In such a way, the prediction error is quantified.

This test is performed using a synthetic signal generated according to equation 8 to sample a sinusoidal motion at $60Hz$, degraded by Gaussian white noise ($SNR = 100dB$).

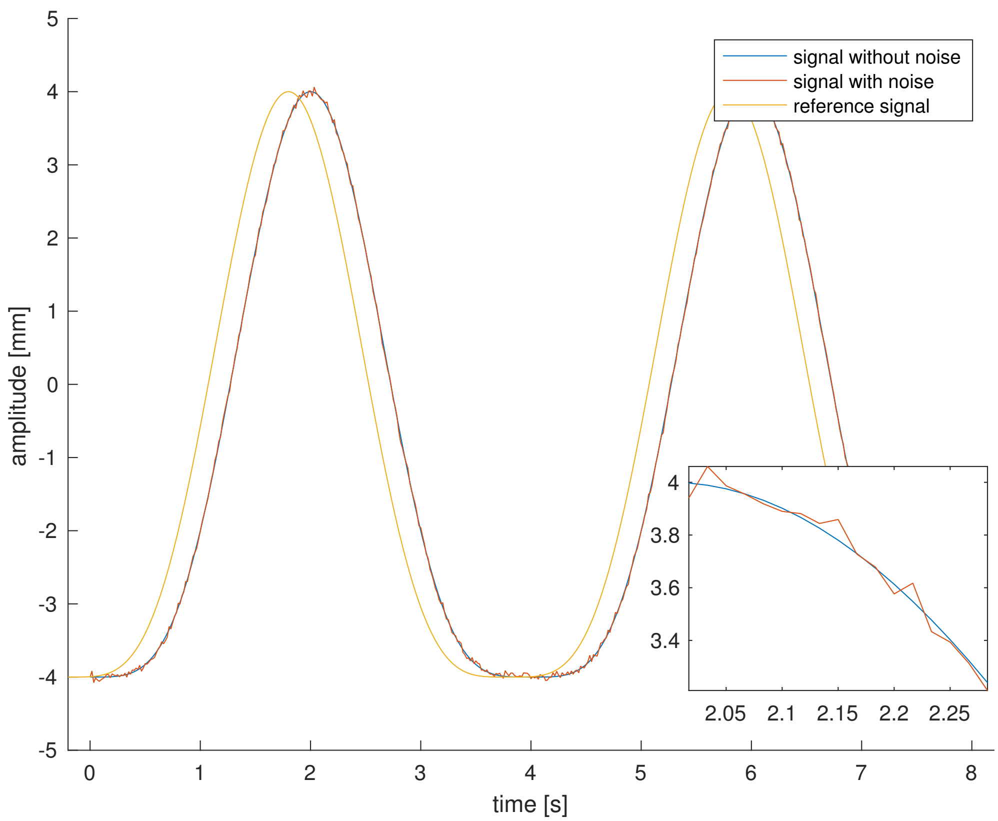

Figure 1: Overlay of reference and input signals. The box in the lower right corner is a zoom of input signal with and without noise addition in the time range between 2.0 and 2.3 seconds.

The full set of trajectories is shown in Figure 1. The prediction step is based on the degraded signal.

$$y_{signal}(t) = 8sin^4(2\pi\frac{t}{8}) - 4 \tag{8}$$

2.1 Amplitude based measures

2.1.1 Root mean square error

Definition The root mean square error, as defined in equation 9, was used to assess the algorithms' geometrical error with respect to the reference signal.

$$RMSE = \sqrt{\sum_{i=1}^{n} \frac{(y_{pred}(t_i) - y_{ref}(t_i))^2}{n}} \tag{9}$$

Results

Parameter optimisation For first and second order polynomial fitting, optimal sample history length were respectively 5 and 20 samples. For the wLMS algorithm, J was set to 11; grid search was performed to identify M and μ (0.01 grid spacing). Figure 2 shows the results for 5 samples prediction horizon. The optimal parameters for all prediction horizons investigated can be found in Table 3. N_{hist} has been chosen large enough to satisfy the condition specified in Table 1 and thus is not listed.
Similarly, a grid search was performed to identify the AOSVR optimal parameters shown in Table 4.

Comparison The algorithms' performance was then compared using the respective optimal parameters (Cfr. Parameter Optimization). Figure 3 shows larger RMSE with increasing prediction horizon. Overall, second order polynomial prediction outperforms the others models despite its significant simplicity. Larger errors for wLMS and SVR approaches are attributable to signal noise. Choosing the noisy signal as reference signal would certainly have resulted in different results. However, because some of the algorithms may overfit the noise the non-degraded signal was used.

prediction horizon[samples]	M	μ	N_{hist} RMSE
1	2	0.38	0.030
5	2	0.31	0.082
10	3	0.35	0.168
20	3	0.38	0.422

Table 3: Results of parameters optimisation for the wLMS algorithm.

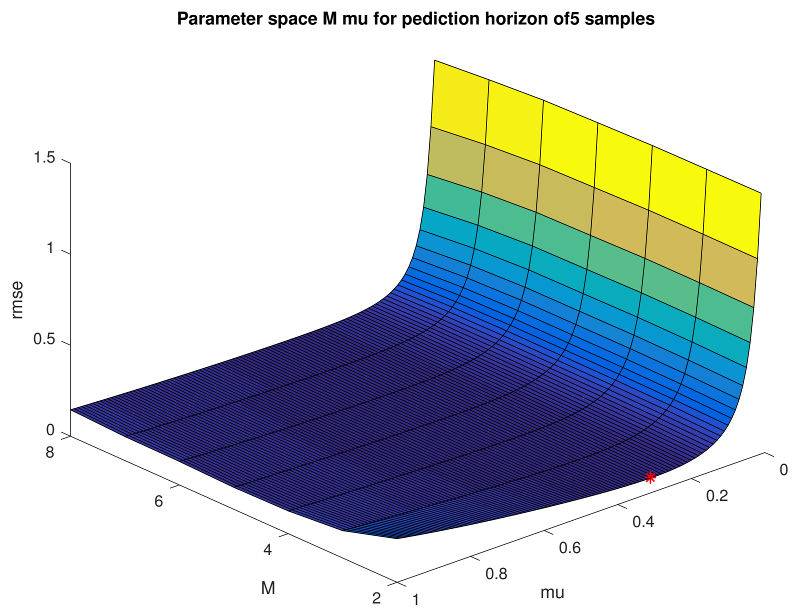

Figure 2: Performance of the wLMS algorithm for different μ and M and prediction horizon of 5 samples. The red star marks the minimum at ($M = 2, \mu = 0.31, RMSE = 0.082$)

prediction horizon[ms]	C	ϵ	Kernel parameter	N_{hist}	RMSE
20	32	0.005	0.42	20	0.0373
60	32	0.003	0.42	20	0.0677
120	32	0.003	0.42	20	0.1399

Table 4: Results of parameter optimisation for the AOSVR algorithm.

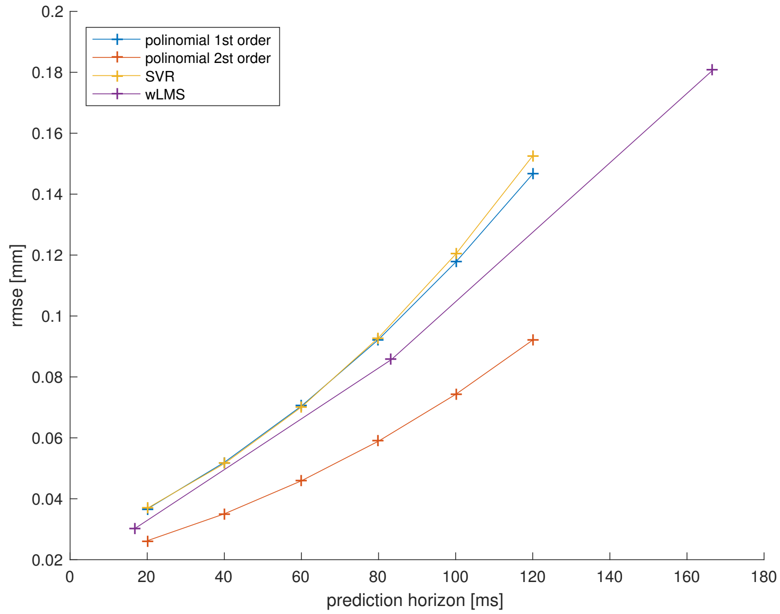

Figure 3: Root mean square error of predicted signals up to 180 msec time prediction.

2.1.2 Jitter

Definition Jitter as defined in equation 10 is basically the average velocity of signals [2]. It quantifies its noisiness. As the perfect predicted signal is not constant, relative jitter was defined as a normalisation of the jitter of the predicted signal with respect to the jitter of the original signal (eq. 11).

$$J(y) = \frac{1}{(N-2)\Delta t} \sum_{i=1}^{N-1} \parallel y_i - y_{i+1} \parallel \tag{10}$$

$$J_{rel}(y, t_{horizon}) = \frac{J(y_{pred})}{J(y)} \tag{11}$$

Results Considering jitter, the second order polynomial predictor outperforms all the alternative models under consideration. In fact, for second order polynomial prediction there is only very little increase in relative jitter with increasing prediction horizon and it hardly exceeds 1. This indicates lower sensitivity to signal noise with respect to other algorithms, i.e. the noise is

less amplified.
The performance of the wLMS algorithm could probably be increased by selecting a larger μ. However, a drawback would be the decrease in RMSE performance.

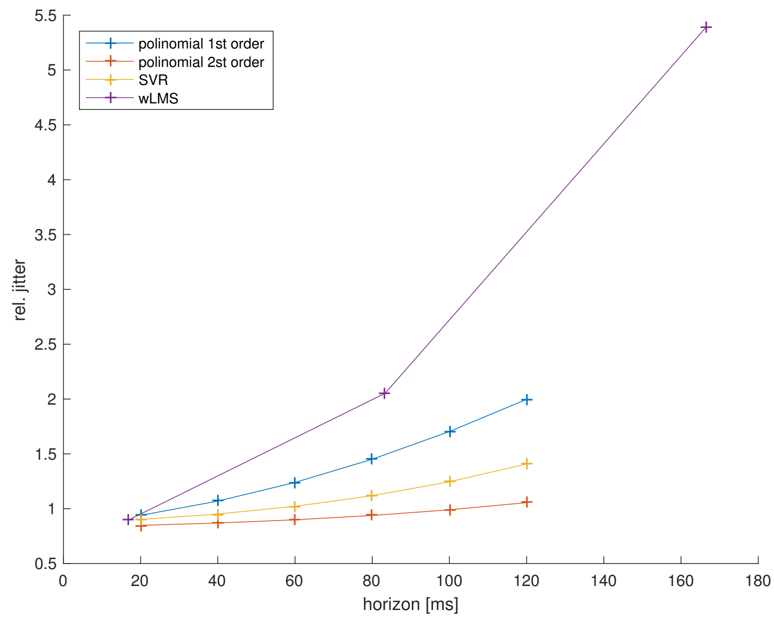

Figure 4: Relative jitter of the predicted signal over the specified prediction horizon. Note that the algorithm's parameters were not optimised for optimal jitter but RMSE.

2.2 Phase based measure

Description Fourier transform was applied to evaluate the result of prediction in the frequency domain. In such a way it is quantified how precisely the model is capable to implement arbitrary prediction horizon. For this purpose, the time delay between the predicted and the input trajectories is quantified by the phase angle difference between the fundamental frequencies of the two signals and compared with the prediction horizon.

Results Large discrepancies between the specified and calculated phase shift were measured. The results summarized in Figure 5 provide a reference

to calibrate prediction horizons.
Accordingly, the evaluation of geometrical error of predicted signals has been updated to express the RMSE with respect to the actual prediction achieved by each method. The results can be seen in Figure 6. Once again, second order polynomial prediction performs better than the other algorithms. Nevertheless, first order polynomial prediction clearly out performs SVR now opposed to the results in Figure 3.

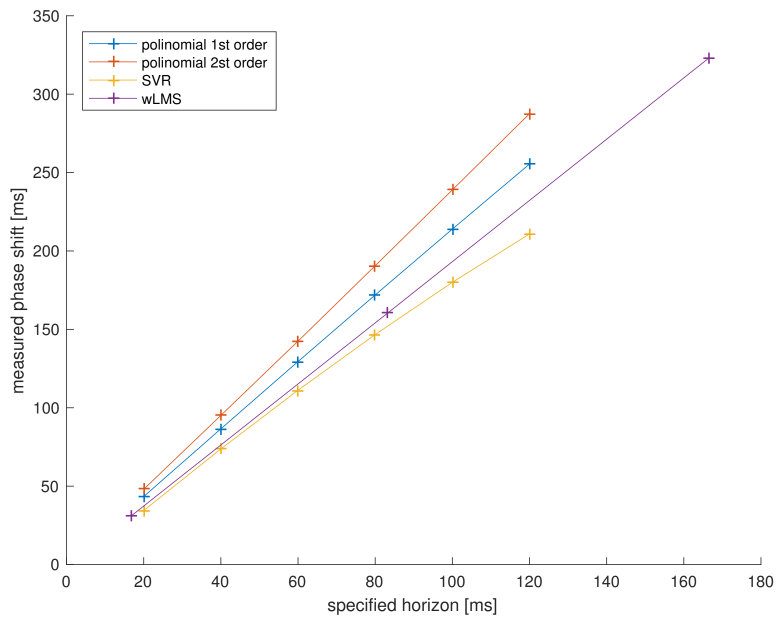

Figure 5: Measured phase shift between predicted signal and actual signal using fast Fourier transform over the specified prediction horizon.

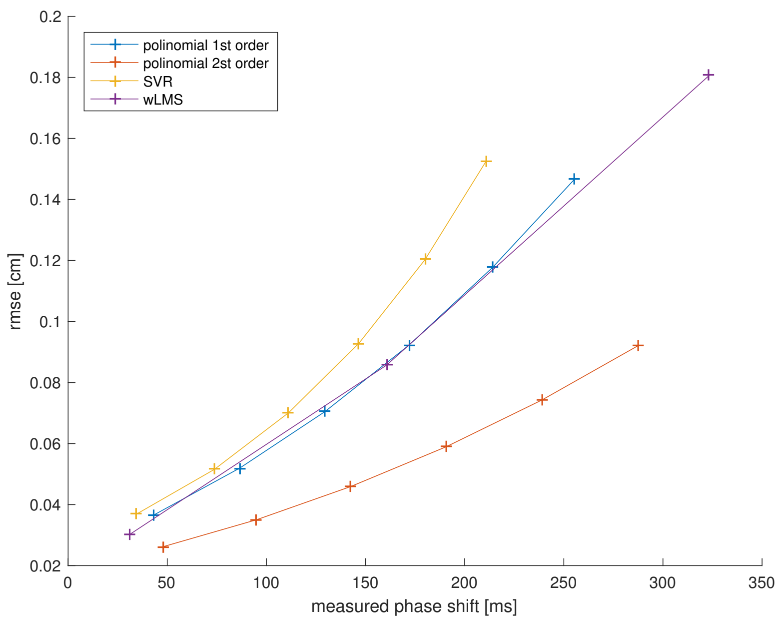

Figure 6: Root mean square error of predicted signal with respect to reference signal over phase shift measured in frequency domain.

2.3 Discussion

Based on this simulation study, second order polynomial prediction represents the best trade-off between computational efficiency and prediction accuracy.
The wLMS, despite its high relative jitter, is fast and accurate enough for small prediction horizons. Its investigation for respiratory motion prediction is worthwhile. Conversely, the SVR, even considering the optimized implementation, was found to be too slow for real-time application. Additional details about the computational cost of wLMS and polynomial prediction can be found in Section 4.

3 On-line respiratory peak detection using time prediction

Polynomial prediction can be applied for on-line peak detection other than latency compensation. Using the absolute error of a first order polynomial

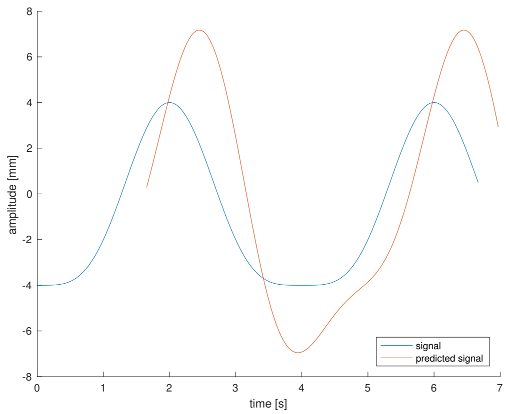

Figure 7: Concept of on-line peak detection. The peak is detected where the predicted signal crosses the original signal.

prediction with relatively large horizon did not yield any advantages compared to simply detecting the peaks with amplitude thresholds.
However, during this investigation it was noted that for long histories and prediction horizon the predicted signal crosses the original signal very close to the peak. A schematic plot illustrating the underlying idea can be found in Figure 7. In fact, this method turned out to be much more stable with respect to changes in period as well as amplitude as shown in Figure 8 where the period of the signal increase from $8s$ to $10s$ and drops to $7s$ afterwards. Simultaneously the amplitude constantly reduces. Despite these changes in the signal, the peaks are detected reliably.
Peaks are significantly easier to detect than valleys. For this reason, the history length ($100samples$) and the prediction horizon ($320ms$) were optimized focusing on the accurate detection of end-inhale peaks, enough to estimate the respiratory frequency of the patient.

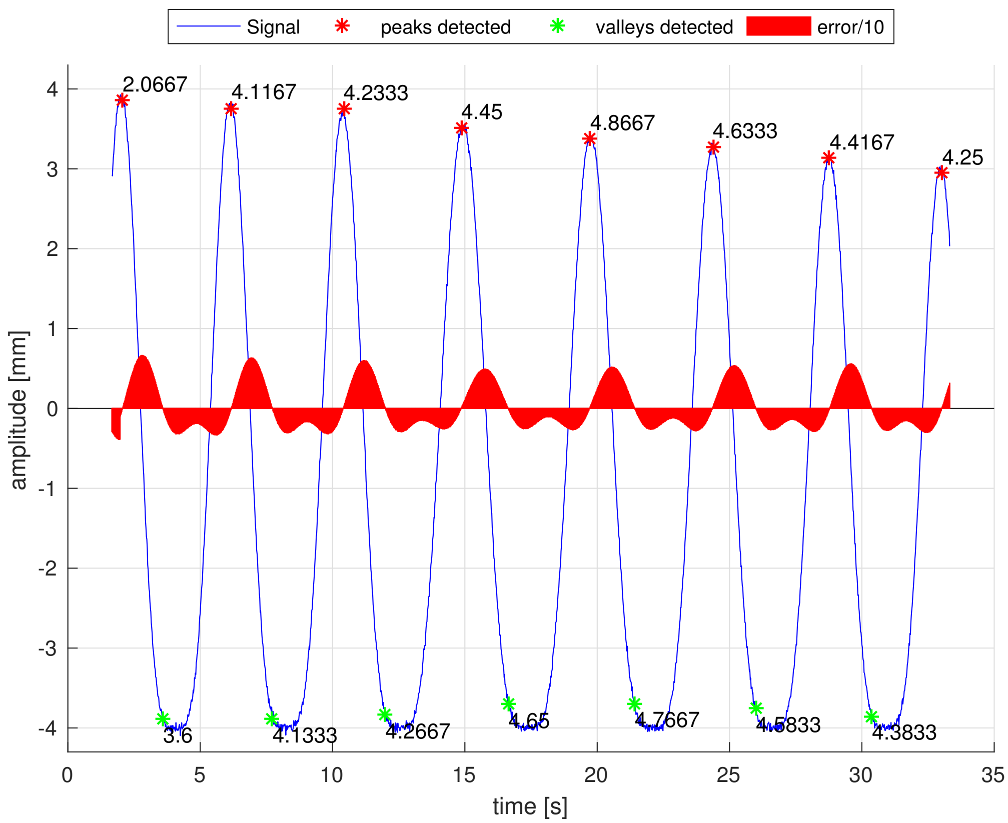

Figure 8: Signal with noise and on-line detected peaks. The numbers next to the detected positions are the times between current and previous detection. The bar plot shows the difference between signal and predicted signal at a given time.

4 Performance of implementation

Polynomial and the wLMS algorithm were implemented in C90 such that they can be integrated into the PSI's gating system [5]. The implementations only rely on standard libraries(string.h, stdio.h, stdlib.h, math.h, stdbool.h, float.h). In addition, the wLMS implementation also requires the BLAS [6] functions dgemm, dscal, dgemv as well as the CLAPACK [1] function dgesvd.

4.1 Results

The execution times were measured in two steps, a training step and a prediction step. The training step is executed every time a new sample is added and ends after the calculation of the coefficients. In the prediction step the current coefficients are used to perform the actual prediction. In principle, it is possible to run the two steps on different threads.
For the time measurement Linux's CLOCK_MONOTONIC was used and the process was scheduled with round-robin algorithm and niceness equal to 98. The testing platform features an Intel® Xeon® Processor E3-1225 v3 and 8GB RAM PC3-10666 (2x4GB) ECC. Figure 9 shows box plots of the measured execution time. As expected prediction is faster than training. In the plot one outlier of $388.49 \mu s$ was omitted for the wLMS training for the sake of clarity. The origin of this outlier remains unclear.

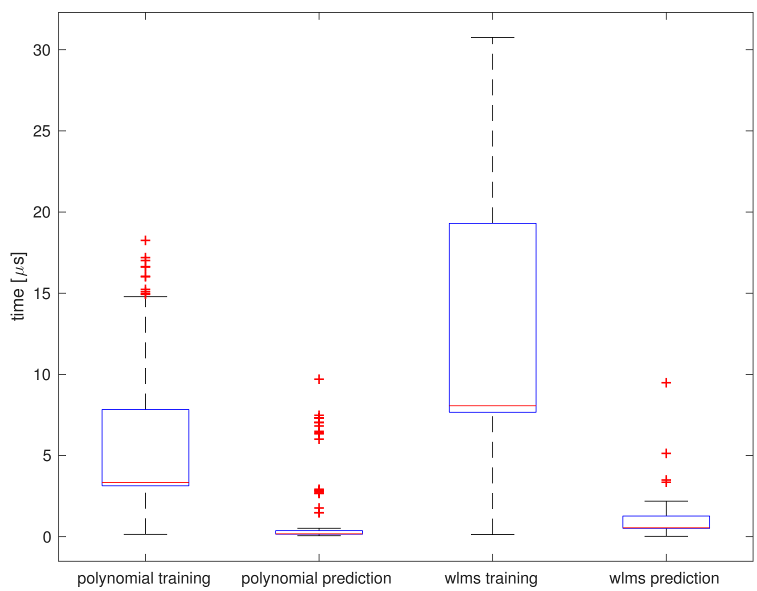

Figure 9: Boxplot of the times for training the polynomial and wLMS prediction algorithm and the prediction step measured using the MONOTONIC clock of UNIX. One outlier($388.49\mu s$) of the wLMS training was not included in the plot for better visibility.

5 Conclusion

Polynomial, wavelet and support vector regression methods were tested for respiratory signal analysis and prediction using a sinusoidal motion trajectory. For each approach, the optimal set of parameters has been estimated and used to quantify geometric and temporal accuracy.
Considering RMSE and computational efficiency, second order polynomial prediction outperforms wLMS and SVR approaches. However, the signal smoothing inherent in wLMS methods saves computational power in those applications where denoising is required.

References

[1] E. Anderson, Z. Bai, C. Bischof, S. Blackford, J. Demmel, J. Dongarra, J. Du Croz, A. Greenbaum, S. Hammarling, A. McKenney, and D. Sorensen. *LAPACK Users' Guide*. Society for Industrial and Applied Mathematics, Philadelphia, PA, third edition, 1999.

[2] F. Ernst, R. Durichen, A. Schlaefer, and A. Schweikard. Evaluating and comparing algorithms for respiratory motion prediction. *Phys Med Biol*, 58(11):3911–3929, Jun 2013.

[3] F. Ernst, A. Schlaefer, and A. Schweikard. Prediction of respiratory motion with wavelet-based multiscale autoregression. *Med Image Comput Comput Assist Interv*, 10(Pt 2):668–675, 2007.

[4] F. Ernst and A. Schweikard. Forecasting respiratory motion with accurate online support vector regression (svrpred). *International Journal of Computer Assisted Radiology and Surgery*, 4(5):439–447, 2009.

[5] G. Fattori et al. Experimental validation of optical tracking of breathing motion for gated treatment with pbs proton therapy. In *Proceedings of ICCR 2016*, 2016.

[6] C. L. Lawson, R. J. Hanson, D. R. Kincaid, and F. T. Krogh. Basic linear algebra subprograms for fortran usage. *ACM Trans. Math. Softw.*, 5(3):308–323, September 1979.

[7] J. Ma, J. Theiler, and S. Perkins. Accurate on-line support vector regression. *Neural Computation*, 15(11):2683–2703, Nov 2003.

[8] F. Parrella. Online support vector regression. Master's thesis, University of Genoa, Italy, 2007.

[9] O. Renaud, J.-L. Starck, and F. Murtagh. Prediction based on a multiscale decomposition. *International Journal of Wavelets, Multiresolution and Information Processing*, 01(02):217–232, 2003.